Geophys. J. Int. (2004) **159,** 565–572 doi: 10.1111/j.1365-246X.2004.02420.x

Sea-surface observations of the magnetic signals of ocean swells

F. E. M. Lilley,[1] A. P. Hitchman,[2] P. R. Milligan[3] and T. Pedersen[4]

[1] *Research School of Earth Sciences, Australian National University, Canberra, ACT* 0200, *Australia. E-mail: Ted.Lilley@anu.edu.au*
[2] *Research School of Earth Sciences, Australian National University, Canberra, ACT* 0200, *Australia. E-mail: Adrian.Hitchman@ukgateway.net*
[3] *Geoscience Australia,* PO Box 378, *Canberra, ACT* 2601, *Australia. E-mail: Peter.Milligan@ga.gov.au*
[4] *Research School of Earth Sciences, Australian National University, Canberra, ACT* 0200, *Australia. E-mail: Tina_Pedersen@wanadoo.dk*

Accepted 2004 April 22. Received 2004 February 20; in original form 2003 June 3

SUMMARY

Ocean swells have a magnetic signal, caused by the motional induction of sea water moving in the steady main magnetic field of Earth. To check the character of such signals at the sea surface, a magnetometer has been set free from a ship to float unrestricted on the surface of the ocean for periods of several days. The path of the floating magnetometer was tracked by satellite; this procedure enabled also the eventual recovery of the magnetometer by the ship.

Superimposed upon a background of slow change of magnetic field, as the magnetometer drifted across different patterns of crustal magnetization, are high-frequency signals generated by the strong ocean swell present at the time. These wave-generated signals are typically up to 5 nT trough-to-peak, consistent with theory for their generation by ocean swells several metres trough-to-peak in height.

The power spectra of the magnetic signals show a consistent peak at period 13 s, appropriate for the known characteristics of ocean swell in the area. The power spectra then exhibit a strong (-7 power) fall-off as period decreases below 13 s. This strong fall-off is consistent with oceanographic observations of the spectra of surface swell, combined with motional induction theory.

Key words: magnetic, motional induction, ocean, signals, swell, waves.

1 INTRODUCTION

A magnetic signal, generated by motional electromagnetic induction, accompanies ocean waves and swell. Sea water moves across the flux lines of the main magnetic field of the Earth and in so doing generates electric currents that flow through the sea water. These electric currents have their own magnetic fields, which are the magnetic fields generated by the wave motion.

To provide sea-surface information on such wave signals, measurements were made in 1998 in the Southern ocean off South Australia. The Southern ocean was a suitable place for the observations, as a result of the presence there of ocean swells, which consistently are several metres in height. The observations were part of the Southern Waters of Australia Geoelectric and Geomagnetic Induction Experiment (SWAGGIE), described by Hitchman (1999) and Popkov *et al.* (2000). Attention had been drawn to the magnetic signals of ocean swell by recent aeromagnetic surveys offshore in Australia (Milligan & Barton 1997) and by the presence of wave signals (both surface and internal) in natural electromagnetic induction data used to study seafloor conductivity structure.

The magnetic fields of ocean waves have been the subject of theoretical investigation by Longuet-Higgins *et al.* (1954), Weaver (1965), Beal & Weaver (1970), Podney (1975), Chave (1984) and Weaver (1997). Maclure *et al.* (1964) and Ochadlick (1989) report measurements in agreement with the theory of Weaver (1965) and observations of the magnetic signals of ocean waves are also reported by Fraser (1966) and Watermann & Magunia (1997). The topic is naturally closely associated with the electric signals of such waves, which are studied in papers such as Cox *et al.* (1978) and Hemer *et al.* (1999). More widely, the topic of electromagnetic induction in the ocean is reviewed by Larsen (1973) and Palshin (1996).

2 THEORY

2.1 Motional induction

Reference is made here to the theory of motional induction of ocean swell as developed by Weaver (1965) and Weaver (1997). An ocean swell is analysed as a simple harmonic wave on the surface of sea water, which is deep in the sense that the depth is much greater than the horizontal wavelength of the wave. The wave propagates in the x direction with wavenumber m and angular frequency ω: the phase speed of the wave c is thus given by

$$c = \omega/m. \tag{1}$$

The magnetic signal $b(x, t)$ in the direction of the main field of Earth (the component measured by a total-field magnetometer) generated

by the ocean swell is then given by

$$b(x, t) = b_F \exp(i\omega t - imx), \tag{2}$$

where t denotes time and b_F, the amplitude of the magnetic signal of the ocean swell, is given by

$$b_F = \frac{Tag\mu_0\sigma F}{8\pi}(\cos^2\theta\cos^2 I + \sin^2 I)\exp(-4\pi^2 h/gT^2). \tag{3}$$

Here, T is the period of the wave (s), a is the amplitude (m), g is the acceleration as a result of gravity, μ_0 is the permeability of free space, σ is the electrical conductivity of the sea water, F is the total magnetic field intensity and I the inclination of the main magnetic field of the Earth, θ is the direction of wave travel measured as an angle positive eastwards from the direction of magnetic north and h is the height of the magnetometer above the sea surface. Introducing a constant K given by

$$K = g\mu_0/8\pi, \tag{4}$$

a geometric function $G(\theta, I)$ given by

$$G(\theta, I) = \cos^2\theta\cos^2 I + \sin^2 I, \tag{5}$$

an exponential decay with height $A(h, T)$ given by

$$A(h, T) = \exp(-4\pi^2 h/gT^2) \tag{6}$$

and notation W for the amplitude of the total-field magnetic signal per unit amplitude of wave given by

$$W = b_F/a, \tag{7}$$

then W may be expressed

$$W = KTF\sigma G(\theta, I)A(h, T). \tag{8}$$

Note that the value of W at the sea surface (for which $h = 0$ and so $A = 1$) is linearly proportional to each of the variables T, F and σ. The reduction of the signal with height above sea surface is exponential and, of the latter three variables, is a function of T only. The height at which the signal falls to $1/e$ of its surface value (the $1/e$ folding height) is given by $gT^2/4\,\pi^2$, that is by $g/\,\omega^2$ where ω is the angular frequency of the wave. For the Southern ocean off South Australia, representative values for F, σ and I are 60 280 nT, 4.4 S m^{-1} and -68.4°, respectively. The electrical conductivity value results from values for surface practical salinity of 35.5 (dimensionless units) and temperature of 16°C taken from maps in Tomczak & Godfrey (1994), combined with tables for the electrical conductivity of sea water in Bullard & Parker (1970). Thus, for the sea surface (taking $g = 9.8$ m s^{-2})

$$W = 0.0176(\cos^2\theta + 6.38)T. \tag{9}$$

This relationship is shown in Fig. 1.

The exponential decrease with altitude for the area will be the quite general one, given for A in eq. (6) and shown as a function of wave period in Fig. 2. Note that in the altitude range 50 to 200 m (a common height for aeromagnetic surveys), the attenuation of the sea-surface signal is considerable and sensitive to the period of the swell.

2.2 Spatial gradients

In the present experiment, the sensor is in motion. The data recorded may thus be affected by the spatial non-uniformity of the ambient magnetic field of the Earth, through which the sensor is moving. Attention will now be given to three possible effects of this sensor motion: (i) oscillation of the sensor up and down with the waves

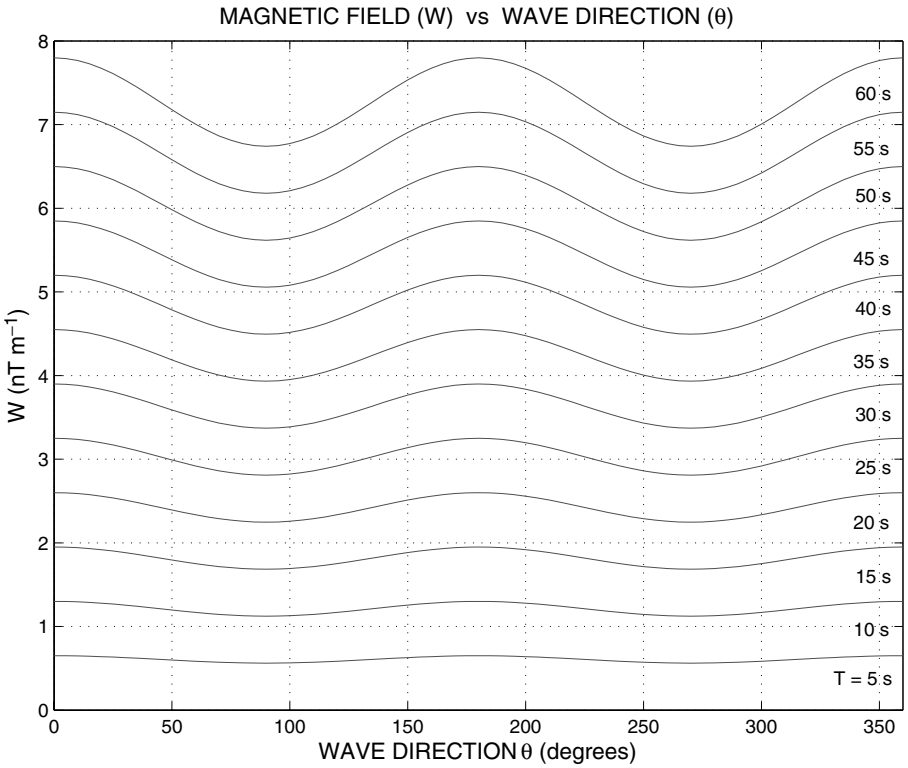

Figure 1. Sea-surface values of swell magnetic signal (W) for different periods of swell, as a function of direction of travel of swell (θ), for the SWAGGIE experiment off South Australia. A maximum period of 60 s has been included to illustrate the behaviour of eq. (9): in practice the local swell periods are less (for example 13 s in the example below).

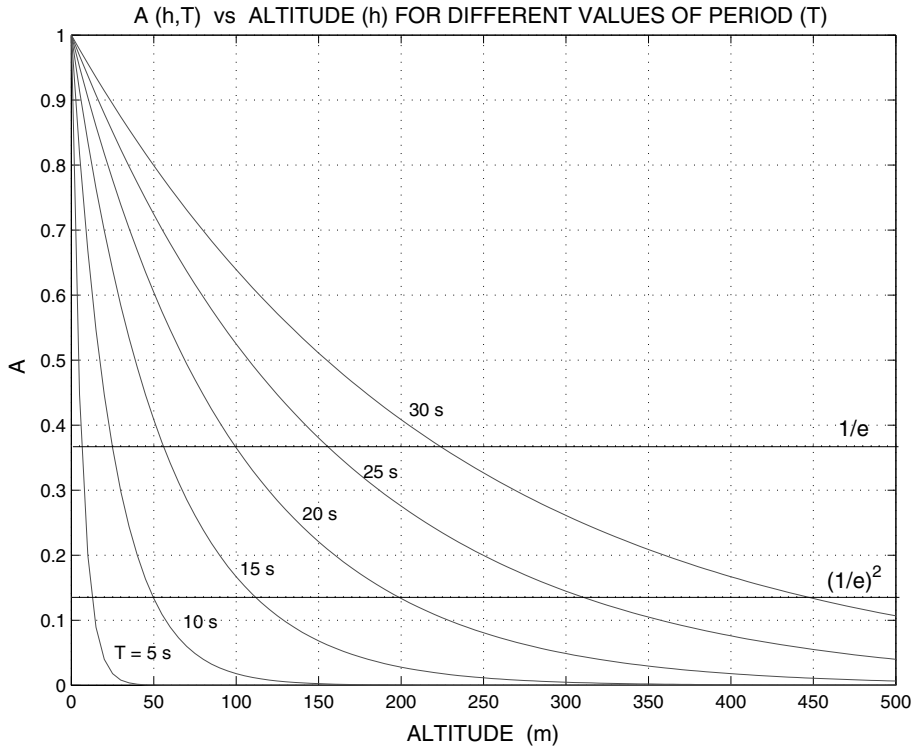

Figure 2. Exponential decrease of swell signal with height of detector above sea surface, for different periods of swell.

themselves; (ii) oscillation of the sensor laterally with the waves; (iii) secular movement of the sensor as a result of its free drift laterally across the geological magnetic pattern of the seafloor.

2.2.1 The dipole field of the Earth

To estimate the effects of the vertical movement, a floating magnetic sensor will move vertically through a distance equal to the wave height (twice the amplitude of the wave). Simple dipole models of the main magnetic field of the Earth predict that the vertical gradient of the total field will be -0.02 nT m^{-1} at the equator and -0.04 nT m^{-1} at the poles. A magnetometer floating in the Southern ocean off South Australia in a swell with height 2 m will thus pick up a spatial signal of order 0.06 nT (trough to peak). While not negligible, this signal is small relative to the motional induction signal, predicted from Fig. 1 to be 3 or 4 nT for a typical swell period of 13 s.

The horizontal gradient of a dipole model for the field of the Earth is everywhere less than the vertical gradient. Zonally the horizontal gradient is zero generally and azimuthally the horizontal gradient has maxima of some 0.006 nT m^{-1} in mid-latitudes between values of zero at the poles and equator. In the ocean off South Australia, a lateral oscillation of say 1-m amplitude in ocean swell will thus cause a spatial gradient magnetic signal of 0.01 nT trough to peak, again small relative to the motional induction signal.

2.2.2 The crustal magnetic field

The magnetic pattern of the crustal rocks over which the magnetometer is floating will also contribute horizontal and vertical gradients in which the magnetometer is oscillated by wave motion. The horizontal gradient in the direction of drift is measured directly by the floating magnetometer and will be evident in data presented below. The steepest horizontal gradient sampled by a floating magnetometer in deep water will there be seen to be 0.01 nT m^{-1} and in more shallow water 0.04 nT m^{-1}. Thus oscillations with amplitude 1 m in such gradients will produce oscillatory signals in the data of amplitudes 0.01 and 0.04 nT, respectively (trough to peak 0.02 and 0.08 nT). While the horizontal gradient perpendicular to the line of drift may differ from that along the line of drift, it would be surprising if it were greatly different.

For vertical gradients, the nearest available aeromagnetic data have been taken, which are for the Eyre Peninsula (see Fig. 3 below). These data have been upward continued to a height of 2000 m to mimic the sensor–source separation for a sensor floating on water 2000 m deep and a map of the vertical gradient of the total-field calculated at that height. A histogram of the vertical gradient values then shows a distribution with a peak at -0.008 nT m^{-1} and with 95 per cent of the values less than 0.06 nT m^{-1} in amplitude. Oscillation of the magnetometer sensor in such a vertical gradient field will give signals that again are small relative to the motional induction signal predicted.

Finally, under the effects of wind and currents, a drifting sensor will traverse the magnetic pattern of the geological crust. As will be seen from the examples presented, the effect of this changing background signal will be to give a slowly changing baseline against which the swell signals are seen. Measured as a change with time, the geologically caused signals are very slow and will not affect time-series analysis of the wave signals.

3 METHOD

On two separate occasions a floating magnetometer (floater-mag) was released from the vessel ORV Franklin and left to float free for approximately 4 days, while the ship carried out other work. The complete floating package also carried a satellite transmitter, so that,

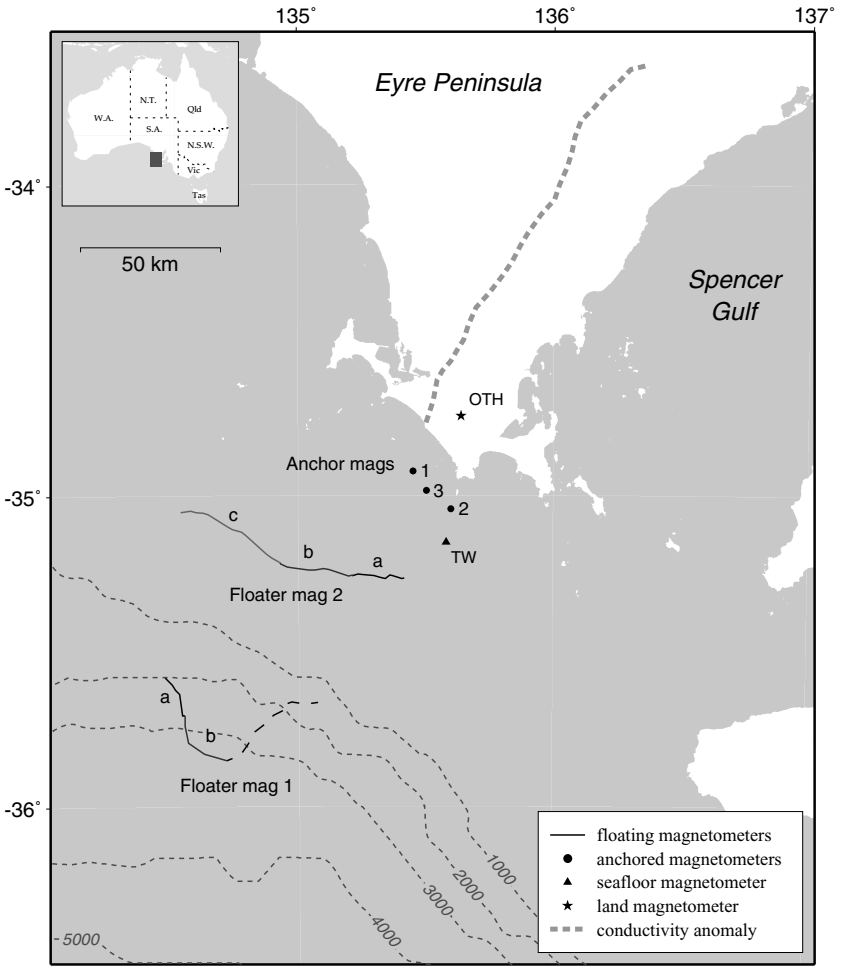

Figure 3. Paths of the two floating magnetometer deployments, floater 1 and floater 2, off South Australia. The land site used as reference, OTH, is shown. Water depth contours are in metres.

as it drifted under the influence of winds and ocean currents, the position of the magnetometer could be tracked and the instrument eventually recovered. Care was taken in the package design to keep the magnetometer itself in a non-magnetic environment and free of stray magnetic fields. A description of the experiment is given in Hitchman *et al.* (2000), in which the floater-mag data are used to determine induction arrows, using a land station as reference. Hitchman *et al.* (2000) note the presence of a swell signal on the floater-mag records.

This paper presents an analysis of the floater-mag data for the swell signal recorded. The paths followed by the drifting magnetometer, termed floater 1 and floater 2, are shown in Fig. 3.

Earlier measurements, testing the equipment, had been made in 1997 in the SODA experiment (Lilley *et al.* 2001). The magnetometer was then tethered to a stationary ship and floated several hundred metres from it downwind.

4 EQUIPMENT

The equipment used was a total-field magnetometer, set up for free-floating marine operation. The recording electronics and power supply were housed in one water-tight sphere and the magnetometer sensor was housed in another, separated 1.8 m from the first by a rigid non-magnetic frame. In the water, a drogue fitted to the magnetometer package kept it upwind of the satellite transmitter, which was tethered at the end of 6 m of buoyant rope. Windage drag on a flag beacon, at the satellite buoy, helped keep the (slightly magnetic) satellite buoy downwind and remote from the magnetometer. The magnetometer took a reading at intervals of 3 s. The magnetometer arrangement was an adaption of, and similar to, the package used by Lilley *et al.* (2001) to make measurements vertically through the ocean column in the East Australian current.

5 RESULTS

5.1 Time-series

Total-field variations recorded by floater-mag, and those from land reference stations, are shown in Fig. 4. The floater-mag time-series have been subdivided for analysis into different lengths and various reference stations have been used, depending on availability. Floater 1 was deployed before the SWAGGIE seafloor and land arrays began recording, thus Canberra Magnetic Observatory is used as a reference station for segment floater 1a in Fig. 4. Data from a seafloor instrument were available for segment floater 1b, but at a lower sampling rate. By the time floater 2 was deployed, the land array of magnetometers had commenced recording, enabling OTH (shown on Fig. 3) to be used as a reference station.

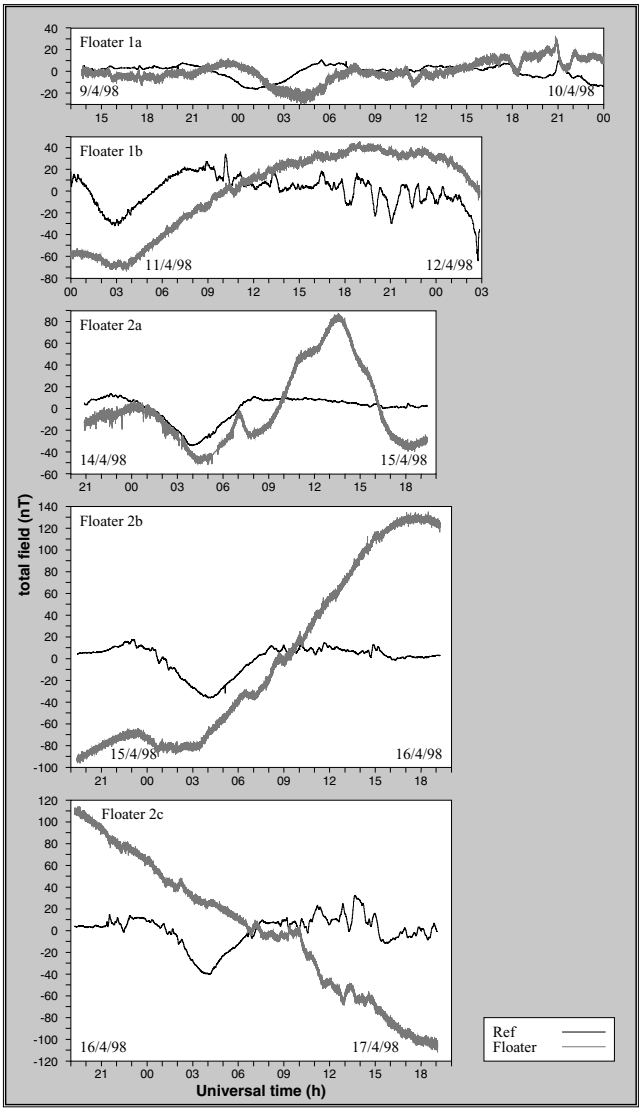

Figure 4. Simultaneous total-field time-series for deployments of the floating magnetometer (thick trace, as a result of the swell signal) and a land reference station (thin trace). The slow drifts of the time-series result from the passage of the floating magnetometer across the crustal magnetic pattern of the seafloor. The land records indicate times of magnetic substorms: these are recorded differently by the floating instrument because of local induction effects (Hitchman *et al.* 2000).

These time-series for the floater-mag deployments show large-scale changes in the total-field occurring slowly, as the instrument drifts across the crustal magnetization pattern. Because floater-mag moved with the ocean currents, its observations record both temporal and spatial total-field variations.

Floater 1 was deployed in deep water (2000–3000 m) and (particularly in floater 1b) the crustal field is evident as a broad anomaly in the time-series. In contrast, floater 2 was deployed above the continental shelf in water approximately 100 m deep and may therefore be more strongly influenced by the crustal anomaly field. There is some evidence in Fig. 4 that the time-series from floater 2 are characterized by larger aperiodic variations than the time-series of floater 1.

Thus, large and slow changes in Fig. 4 are the result of the magnetometer moving across the crustal magnetization patterns of the seafloor, as it was carried by ocean currents and winds. However, when the time-series from the floater-mag are expanded, a short-period signal is consistently evident. The signal is variable in amplitude, typically ranging up to 5 nT in trough-to-peak value. An example is shown in Fig. 5.

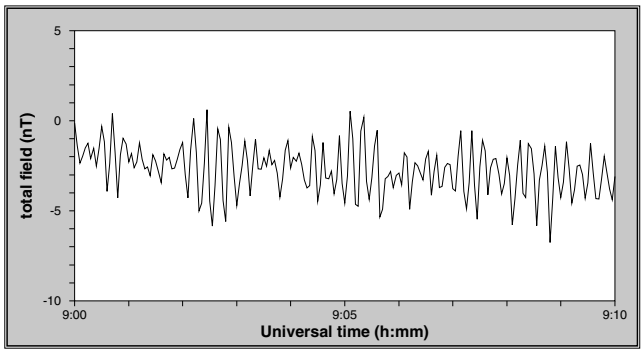

Figure 5. Example of time-series for floater 1a over a period of 10 min, showing the magnetic signals of individual ocean swells. The zero level for the magnetic field is arbitrary. The significant signal height for this example is 4.6 ± 0.2 nT.

Adapting, to Fig. 5, the oceanographic concept that a significant signal height is the mean height of the one-third highest waves (Pond & Pickard 1983), a significant signal height for the data in Fig. 5 is calculated to be 4.6 nT, with a standard error of 0.2 nT.

5.2 Power spectra

Power spectra for each of the floater-mag time-series are presented in Fig. 6, together with spectra for the same variations recorded at each of the reference stations. The important feature, for the purposes of the present paper, is the consistent peak in all the floater-mag spectra at approximately 13 s. It is this spectral peak that corresponds to the swell signal and that will now be examined more carefully.

It should at this stage be mentioned that *Pc*3 pulsations occur naturally in the geomagnetic field over a period range that includes 13 s (Campbell 1997) and that circumstances could arise in which such pulsations confuse the recognition of the magnetic signal of ocean swell. In the present case however such pulsations would not be expected to occur continuously over days as shown in Fig. 4, or have the clear spectral peak shown by the floater-mag data in Fig. 6. Further, inspection of the Canberra Magnetic Observatory record for the time of Fig. 5 shows no particular pulsation activity and note that the observatory records show no spectral peak at 13 s in the top left panel of Fig. 6. There is thus no reason to attribute the signal in Fig. 5 to geomagnetic pulsations.

The swell signal is thus ubiquitous in the floater-mag data, and attention is now focussed particularly on the records of floater 1. The reason is that as a result of their observation in deeper water, these data satisfy more exactly the condition adopted in the theory of an infinitely deep ocean. In contrast, for floater 2 data, the ocean depth of 100 m is of the same order of magnitude as the wavelength of the swell. Another benefit of the deep-water data is the lesser magnetic gradients at the surface as a result of the crustal magnetic pattern.

A power spectrum for the entire time-series of floater 1 is shown in Fig. 7. The power spectrum shows a clear peak in power at 13.3 s, caused by the ocean swell. The period of the swell found in this analysis corresponds closely to the findings of Hemer & Bye (1999)

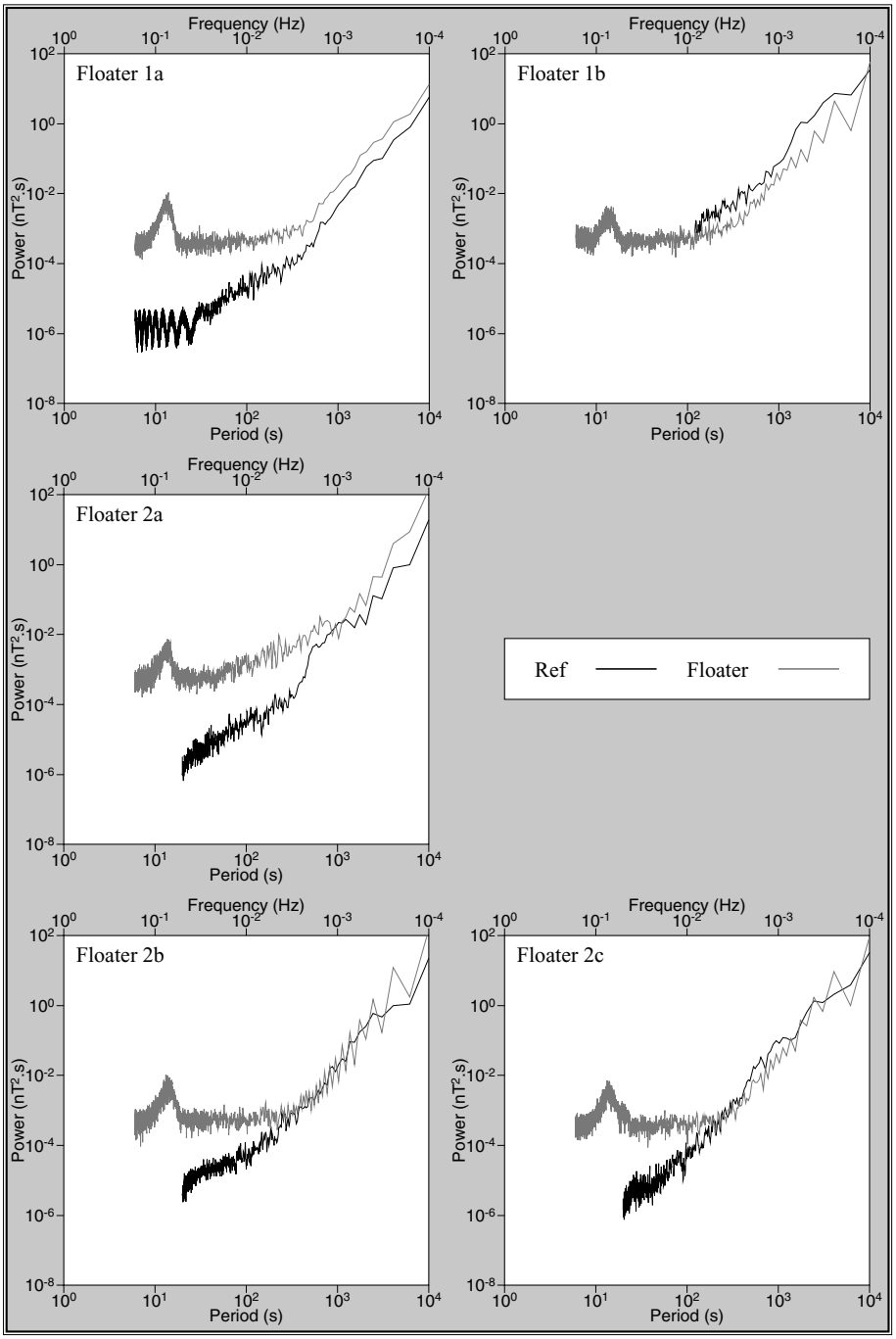

Figure 6. Power spectra for the floater-mag total-field variations, together with similar spectra for the land reference stations. Except for floater 1a, for which the land reference is Canberra Magnetic Observatory, the land-station data have a lesser digitizing interval than the floater data, so their power spectra do not go to periods as short as the swell period (13 s). However, the ubiquity of the peak in the floater spectra at the swell period of 13 s is clear, as is the absence of land data signal at this period.

and Hemer *et al.* (1999) for the swell period in the South Australian sea in 1998 April.

Under many circumstances the wave-energy spectrum of the ocean is approximately represented by the Phillips spectrum (Phillips 1977). The Phillips spectrum has a characteristic fall-off with frequency of power -5. Inspection of eq. (3) shows that if a^2, representing the power of the swell, has a frequency dependence of -5, then $b_F{}^2$ will have a frequency dependence of -7, as the T in eq. (3), when squared, will contribute a further factor of ω^{-2}.

Thus, for signals measured by total-field magnetometers, a fall-off with frequency with a theoretical slope of -7 is predicted for the power. A double logarithmic plot of the power versus the frequency of the magnetic signal shows this phenomenon well, see Fig. 7.

6 DISCUSSION

It is a straightforward explanation of the fluctuations seen in Fig. 5 that they are magnetic variations associated with ocean swell. The

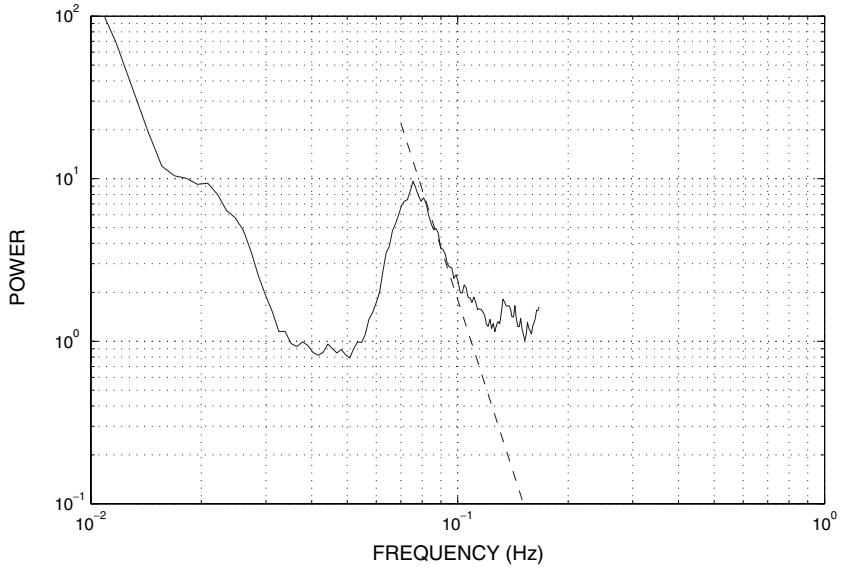

Figure 7. Power spectrum for the deep-water floater 1 time-series of total magnetic field, plotted with a line of slope −7 as predicted by theory.

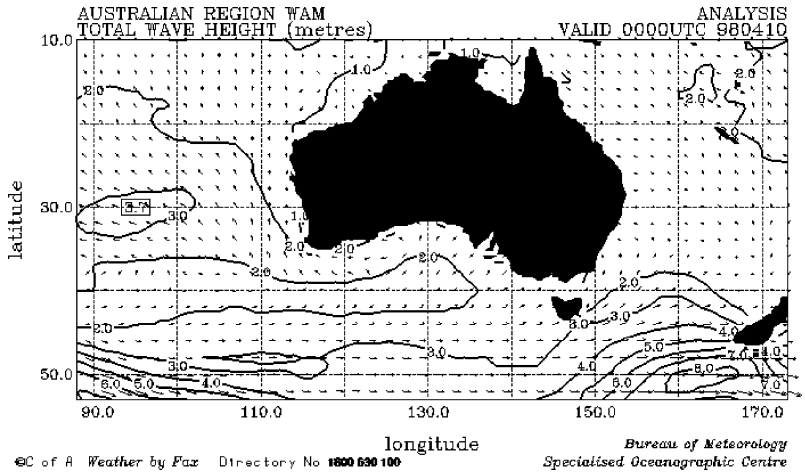

Figure 8. Map of significant wave height (swell plus wind waves) and swell direction forecast on the basis of numerical modelling for the time of the floating magnetometer observations shown in Fig. 5. Nominally, the time is 00 00 h UT on 1998 April 10. For the SWAGGIE area, the swell direction is 45° geographic (i.e. 39° magnetic) and the significant swell height is in the range 2 to 3 m.

pattern in Fig. 5 shows packets of waves, of varying heights, as are known to occur in practice. Weather forecasts at the time by the Australian Bureau of Meteorology model a swell height of between 2 and 3 m for that part of the Southern ocean, as shown in Fig. 8, and a direction of swell travel of 45° geographic (39° magnetic). Global hindcast data from the NOAA Wavewatch III internet site (http://polar.ncep.noaa.gov/waves) give a swell period of 13 s for the area at the time in question, in agreement with the spectral peaks observed.

The values of 39° for θ and 13.3 s for T may now be used in eq. (9) to give a value for W of 1.63 nT m^{-1}. This value, combined with the result from Fig. 5 of a significant magnetic signal height of 4.6 ± 0.2 nT, gives a significant swell height of 2.8 ± 0.1 m. The swell height predicted for the SWAGGIE area in Fig. 8 is seen to be greater than 2 m and less than 3 m, so that there is agreement within the approximate nature of Fig. 8.

The agreement suggests that a floating total-field magnetometer, which has no moving parts, may be a simple independent way of monitoring swell heights in the open ocean. Further tests where control information on actual swell heights is available would be valuable. Further refinements would include observations over continental shelves, where the nature of the waves should change (being no longer deep-water waves) and an investigation of the effects of the electrical conductivity of the water diminishing with depth, as temperature reduces.

For some purposes, such as aeromagnetic surveying, the magnetic signal of ocean swell is a source of error and it is well appreciated that a way to suppress such signals is by increasing the height of measurement above the sea surface. The exponential decay of the swell signal with height is then straightforward and the 1/e folding height is a function of swell period only. With such a strategy, the benefits of suppressed swell signal are offset by reduced definition of the observed magnetic pattern, which is also a consequence of increasing height.

However, an important result of the present work has been to demonstrate the −7 power fall-off of the magnetic signal with

increasing frequency. This phenomenon causes the magnetic signal to have a narrow frequency band. When the ocean swell has travelled some distance from its place of origin, this result should apply quite generally. Such an implied sharp spectral peak in the swell magnetic signal may aid its filtering in aeromagnetic and other applications of marine magnetic measurements.

7 CONCLUSIONS

A research cruise off the coast of South Australia has provided an opportunity to observe the magnetic signals of ocean swell, generated by motional induction. The place of the experiment has been favourable, as a result of the occurrence there of swell generated by the storms of the Southern ocean. Magnetic signals measured by a magnetometer floating freely on the surface of the Southern ocean are of the correct form to be created by an ocean swell of period 13 s and height several metres. The constant of proportionality in the generation process as predicted by Weaver's theory is approximately 1.6 nT of magnetic signal for every 1 m of wave motion.

The sharp peak in the signal spectrum at 13-s period decreases very strongly with increasing frequency, consistent with a prediction from physical oceanography. The results of the experiment suggest that a floating total-field magnetometer, which has no moving parts, may be a simple independent way of monitoring swell heights in the open ocean.

ACKNOWLEDGMENTS

We thank our collaborators in the SWAGGIE project and the captain and crew of ORV Franklin (cruise FR04/98) for their contributions to the work presented in this paper. We thank John Bye for the benefit of discussions during his visit to Canberra in 2000.

The magnetometer set up in the floating package was a GEM Systems GSM-19 Overhauser magnetometer. The satellite transmitter used to track the floating magnetometer was part of the Argos system. The software of Wessel & Smith (1995) has been used in the preparation of this paper. APH carried out his part of the work while supported by an ANU Research Scholarship. TP carried out her part of the work while a visiting scholar at ANU. PRM publishes with the permission of the Executive Officer, Geoscience Australia. Karen Weitemeyer is thanked for her help in the preparation of the paper. We have benefitted from discussion with Graham Warren of the Australian Bureau of Meteorology, who is thanked for supplying Fig. 8. We thank Jean Francheteau, Rob Tyler and an anonymous reviewer for comments that have improved this paper.

REFERENCES

Beal, H.T. & Weaver, J.T., 1970. Calculations of magnetic variations induced by internal ocean waves, *J. geophys. Res.,* **75**, 6846–6852.

Bullard, E.C. & Parker, R.L., 1970. Electromagnetic induction in the oceans, in, *The Sea*, Vol. 4, pp. 695–730, ed. Maxwell, A.E., Wiley-Interscience, New York.

Campbell, W.H., 1997. *Introduction to Geomagnetic Fields,* Cambridge Univ. Press, Cambridge.

Chave, A.D., 1984. On the electromagnetic fields induced by oceanic internal waves, *J. geophys. Res.,* **89,** 10 519–10 528.

Cox, C.S., Kroll, N., Pistek, P. & Watson, K., 1978. Electromagnetic fluctuations induced by wind waves on the deep sea floor, *J. geophys. Res.,* **83,** 431–442.

Fraser, D.C., 1966. The magnetic fields of ocean swell, *Geophys. J. R. astr. Soc.,* **11,** 507–517.

Hemer, M.A. & Bye, J.A.T., 1999. The swell climate of the South Australian sea, *Trans. R. Soc. South Aust.,* **123,** 107–113.

Hemer, M.A., Heinson, G.S., Bye, J.A.T. & White, A., 1999. Wave energy turbulence spectra from the measurement of electric fields in the ocean, in, *The wind-driven air-sea interface,* pp. 49–56, ed. Banner, M.L., Univ. of NSW, Sydney.

Hitchman, A.P., 1999. Interactions Between Aeromagnetic Data and Electromagnetic Induction in the Earth, *PhD thesis,* The Australian National University, Canberra.

Hitchman, A.P., Lilley, F.E.M. & Milligan, P.R., 2000. Induction arrows from offshore floating magnetometers using land reference data, *Geophys. J. Int.,* **140,** 442–452.

Larsen, J.C., 1973. An introduction to electromagnetic induction in the ocean, *Phys. Earth planet. Int.*, **7,** 389–398.

Lilley, F.E.M., White, A. & Heinson, G.S., 2001. Earth's magnetic field: ocean current contributions to vertical profiles in deep oceans, *Geophys. J. Int.,* **147,** 163–175.

Longuet-Higgins, M.S., Stern, M.E. & Stommel, H., 1954. The electric field induced by ocean currents and waves, with applications to the method of towed electrodes, *Pap. Phys. Oceanogr. Meteorol.,* **13,** 1–37.

Maclure, K.C., Hafer, R.A. & Weaver, J.T., 1964. Magnetic variations produced by ocean swell, *Nature,* **204,** 1290–1291.

Milligan, P.R. & Barton, C.E., 1997. *Transient and induced variations in aeromagnetics*, Records of Australian Geological Survey Organization Vol., **27,** AGSO, Canberra.

Ochadlick, A.R., 1989. Measurements of the magnetic fluctuations associated with ocean swell compared with Weaver's theory, *J. geophys. Res.,* **94,** 16 237–16 242.

Palshin, N.A., 1996. Oceanic electromagnetic studies: a review, *Surv. Geophys.,* **17,** 455–491.

Phillips, O.M., 1977. *The dynamics of the upper ocean,* Cambridge Univ. Press, Cambridge.

Podney, W., 1975. Electromagnetic fields generated by ocean waves, *J. geophys. Res.,* **80,** 2977–2990.

Pond, S. & Pickard, G., 1983. *Introductory Dynamical Oceanography,* 2nd edn, Pergamon Press, Oxford.

Popkov, I., White, A., Heinson, G., Constable, S., Milligan, P. & Lilley, F.E.M., 2000. Electromagnetic investigation of the Eyre Peninsula conductivity anomaly, *Explor. Geophys.*, **31,** 187–191.

Tomczak, M. & Godfrey, J.S., 1994. *Regional Oceanography: an Introduction,* Pergamon Press, Oxford.

Watermann, J. & Magunia, A., 1997. Propagation parameters of sea surface waves inferred from observations from two closely spaced vector magnetometers, *J. Geomagn. Geoelectr.*, **49,** 709–720.

Weaver, J.T., 1965. Magnetic variations associated with ocean waves and swell, *J. geophys. Res.,* **70,** 1921–1929.

Weaver, J.T., 1997. Generation of magnetic signals by waves and swells, in, *Transient and induced variations in aeromagnetics,* Records of Australian Geological Survey Organization vol., **27,** Australian Geological Survey Organization, pp. 15–16, eds Milligan, P.R. & Barton, C.E., AGSO, Canberra.

Wessel, P. & Smith, W.H.F., 1995. New version of the Generic Mapping Tools released, *EOS, Trans. Am. geophys. Un.*, **76,** 329.